

Inter-Modality Non-Rigid Breast Image Registration Using Finite-Element Method

Andrzej Krol, *Member, IEEE*, Ioana L. Coman *Member, IEEE*, James A. Mandel, Karl Baum, Min Luo, David H. Feiglin, Edward D. Lipson, and Jacques Beaumont

Abstract—We have investigated a new approach for co-registration of functional PET images with anatomical MR images for breast-cancer detection. This registration is required for multimodality PET-MRI breast image fusion, an approach that could prove useful as an alternative to surgical breast biopsy, following equivocal or difficult-to-interpret mammograms. Our method uses fiducial skin markers placed on the breast that can be observed in PET and MRI. The intermodal geometrical displacements (i.e. differences between PET and MRI marker locations) are estimated from tomographic images. A finite-element-method (FEM) model of breast tissue, based upon an analogy between the orthogonal components of the displacement field and a steady-state heat transfer (SSHT) problem was implemented. This equivalence is valid in that the displacement distribution problem is analogous to the SSHT in solids. The material properties of the breast appear here as coefficients of “thermal conductivity.” Our model considers the observed marker displacements as FEM “temperature loads” and distributes them linearly (stepwise) over the entire breast volume. To test the performance of our method, an elastic breast phantom with simulated internal “lesions” and external markers placed on

four meridians was imaged with PET and MRI. We estimated fiducial-registration errors and target-registration errors in the PET-MRI co-registration. The effects of the number, location, and distribution of the markers on the accuracy of the procedure were also investigated. We have established that multimodality breast-image co-registration using our SSHT FEM approach with external fiducial markers is accurate to within ~ 5 mm.

I. INTRODUCTION

THE normal follow-up diagnostic treatment following equivocal or difficult-to-interpret screening mammography is surgical biopsy. Since about half of breast biopsies turn out negative [1], it would be highly desirable to have an alternative, noninvasive approach as the second line of defense after mammography. To that end, we have embarked on developing a 3D FEM-based model for calculation of the entire displacement field in the breast from known displacements of external fiducial markers visible in both PET and MRI. This model is used for non-rigid co-registration of two multimodality (PET and MRI) breast-image volumes.

II. MATERIALS AND METHODS

A. Phantom

A custom-manufactured deformable breast phantom (CIRS Inc., Norfolk, VA; www.cirsinc.com) consisted of a medium-stiffness gel (vinyl-based hydrogel with low concentration of nickel chloride) surrounded by a skin made of thin urethane foil (Figs. 1 and 2).



Fig. 1. Deformable breast phantom. *Left*: supported on its base. *Right*: suspended in orientation used in experiments. The diameter (neglecting the base) is approximately 10 cm. See text for details.

Manuscript received October 31, 2003.

A. Krol is with the Department of Radiology, SUNY Upstate Medical University, Syracuse, NY 13210 USA (telephone: 315-464-7054, e-mail: krola@upstate.edu).

I. L. Coman is with the Department of Mathematics and Computer Science, Ithaca College, Ithaca, NY 14850 USA (telephone: 607-274-5704, e-mail: icoman@ithaca.edu).

J. A. Mandel is with the Department of Civil and Environmental Engineering, Syracuse University, Syracuse, NY 13244 USA (telephone: 315-443-3041, e-mail: jmandel@syr.edu).

K. Baum is with the Department of Electrical Engineering and Computer Science, Syracuse University, Syracuse, NY 13244 USA (telephone: 315-443-3041, e-mail: kgbaum@ecs.syr.edu).

M. Luo was with Syracuse University. She is now with the Department of Biomedical Engineering, University of Wisconsin, Madison WI 53706 USA (telephone: 608-263-4660, e-mail: miluo@wisc.edu).

D. H. Feiglin is with the Department of Radiology, SUNY Upstate Medical University, Syracuse, NY 13210 USA (telephone: 315-464-7061, e-mail: feiglind@upstate.edu).

E. D. Lipson is with the Department of Physics, Syracuse University, Syracuse, NY 13244 USA (telephone: 315-443-3901, e-mail: edlipson@syr.edu).

J. Beaumont is with the Department of Pharmacology, SUNY Upstate Medical University, Syracuse, NY 13210 USA (telephone: 315-464-7980, e-mail: beaumontj@upstate.edu).

B. Markers and Lesions

Fiducial skin markers (Fig. 2), containing modality-specific material (Magnavist for MRI and F-18-FDG for PET), were placed in indicated positions along four orthogonal meridians, as well as at the apex (i.e. where human nipple would be). Out of 33 markers placed, 27 could be correctly identified in both modalities.

Simulated “lesions” were introduced by injection of oil (Johnson & Johnson; non-diffusing in the gel) containing a mixture of organic azo dyes (less than 5% by weight). For PET scans, the radioactive material (diluted in water-soluble gelatin with organic dyes) was injected as closely as possible to the “lesions.” For both MRI and PET, 13 lesions were introduced. Of these, six internal lesions were correctly identified in common for both modalities.

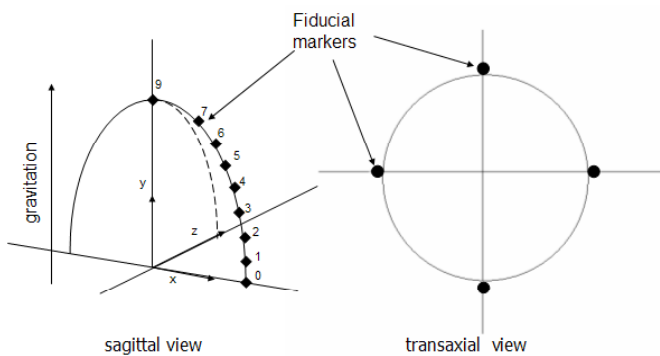


Fig. 2. Placement of external markers on surface of deformable breast phantom. Eight markers are placed on each four meridians and one additional marker is placed on the apex, for a total of 33.

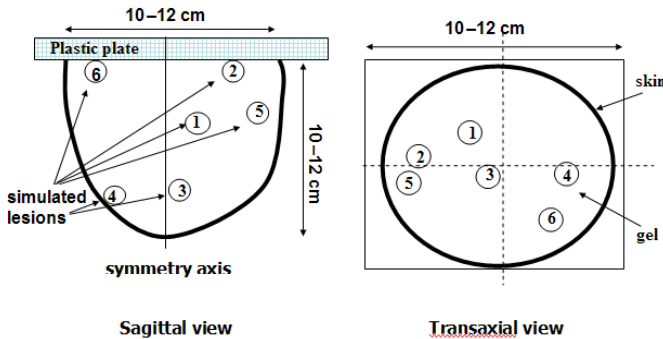


Fig. 3. Representative placement of “lesions” inside deformable breast phantom.

C. Imaging Modalities

This study employed F-18 FDG positron emission tomography and high-resolution magnetic resonance imaging (Table I).

TABLE I
IMAGING SPECIFICATIONS

	MRI	PET
Scanner	Philips 1.5 T, Intera	GE Advance
Scan parameters	T1-weighted isotropic 3D FFE sequences with flip angle 20°	Transmission scan 3 min Emission scan 5 min
Spatial resolution	0.7 mm	<7 mm
Acquisition/reconstruction matrix	512 × 512	128 × 128
Voxel size	0.7 × 0.7 × 1.12	4.25 × 4.25 × 4.25

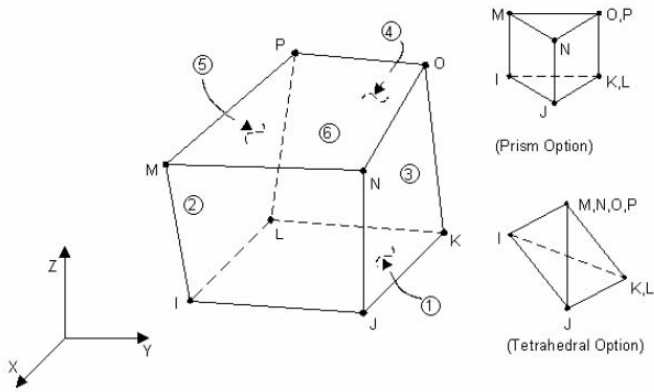
D. Multimodality Registration Using Finite Element Method

For the co-registration, we employed finite-element method (FEM) to generate a 3D finite-element model of the breast phantom. Accordingly, displacements (between PET and MRI images) for every location within the phantom were obtained via FEM from observed displacements of fiducial skin markers. The FEM computations used the ANSYS FEM software package (ver. 5.7; ANSYS, Inc., Canonsburg, PA, www.ansys.com).

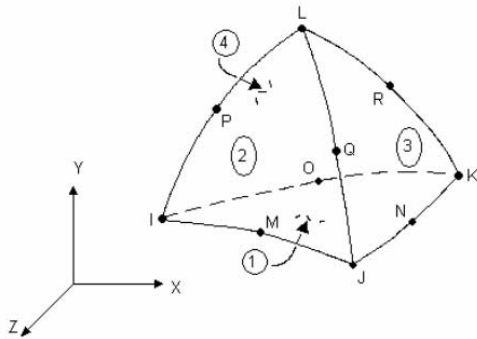
We assumed unchanged stress conditions, because a) phantom positioning is maintained well in the two imaging systems, and b) fiducial-marker positioning is essentially identical for both modalities. In other words, we have assumed, in applying FEM, that there are *no stress-induced deformations*.

For convenience, our FEM treatment of image registration, using ANSYS, is modeled as a steady-state heat-transfer (SSHT) problem. The displacement components are mathematically equivalent to temperature differences in SSHT. Since temperature is a scalar, it is taken, in turn, to represent each of the three spatial dimensions. Loads u_x , u_y , u_z , representing displacements at fiducial-marker locations, are all distributed linearly over the phantom domain.

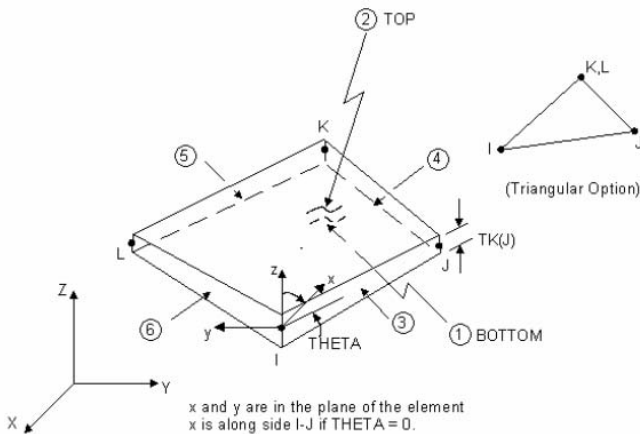
To build the geometry of the breast, high-resolution MRI was used. For meshing and analysis, the following elements were chosen from the ANSYS library: *SOLID87* 3-D 10-node tetrahedral thermal solid; *SOLID70* 3-D thermal solid; and *SHELL57* 2-D thermal shell (Fig. 4). A mesh containing a total of 15,636 nodes was created. *SOLID87* and *SOLID70* elements were used in the bulk of the object. The surface was meshed by a layer of *SHELL57* elements. Thermal conductivity assigned to these surface elements was 1,000 times that used in the bulk of the phantom. This has the desired effect that the surface layer reaches steady state 1,000 times faster than the interior. The execution time was 20 s per Cartesian component for the entire mesh (using a 3 GHz, dual Xeon processor PC).



SOLID70 3-D Thermal Solid



SOLID87 3D 10-Node Tetrahedral Thermal Solid



SHELL57 Thermal Shell

Fig. 4. The three ANSYS models used in this study (from ANSYS user manual).

III. RESULTS

Figure 2 shows representative images from PET and MRI.

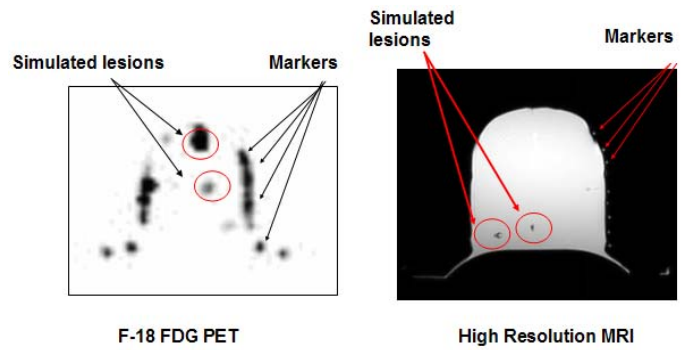


Fig. 5. PET (left) and MR (right) images showing some of the markers and “lesions” (targets). Some lesions were placed deep in the interior, while others were beneath the surface (some near markers and others more distant).

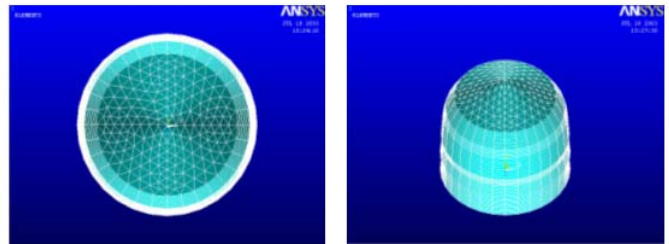


Fig. 6. FEM mesh generated by ANSYS software. *Left*: top view. The outer ring (white) shows shell elements. The inner ring shows brick elements. The central (and uppermost) area has tetrahedral elements. *Right*: oblique view. Brick elements are visible on the sides, and tetrahedral elements at and near the top.

We tested the hypothesis that the internal stress conditions in the simulated breast are practically the same in all imaging modalities, because of similar phantom (patient) positioning in the imaging systems. We conjectured that image differences between the modalities are mainly produced by image distortions created in the imaging process and rigid transformations (scaling, rotation, translation). For both modalities, the fiducial markers were placed in the same locations (permanently marked) on the simulated breast skin. We adopted the analogy between the orthogonal components of the displacement field and a steady-state temperature.

We considered two error measures: fiducial-registration error (FRE), and target-registration error (TRE); see Tables II and III, and Fig. 7. TRE is estimated in the interior lesion area, and FRE is estimated for the surface fiducial markers that were excluded from the registration process. The co-registration FEM-based procedure, using external fiducial markers, is accurate to within ~5 mm (voxel size in PET). TRE can be as large as two PET voxels, if the “lesion” is not surrounded by proximal fiducial markers.

TABLE II
FIDUCIAL REGISTRATION ERRORS¹

No. of markers used in the FEM model	Mean Error	Standard Deviation	Min Error	Max Error
13	4.06	1.55	2.32	9.94
8	4.27	2.16	1.55	1.55
27 (all)	0.00007	0.00008	0.00002	0.00038

¹Fiducial registration errors (FRE, in mm) estimated using selected fiducial markers not used in the FEM model calculation for PET-MR co-registration. A total of 27 identifiable markers were available.

TABLE III
TARGET REGISTRATION ERRORS, USING ALL MARKERS¹

Lesion	x_{obs}	x_{est}	y_{obs}	y_{est}	z_{obs}	z_{est}	TRE
1	1.05	1.19	0.51	-0.91	-9.40	-4.69	4.92
2	1.99	0.29	2.15	-0.92	-6.49	-3.53	4.58
3	-1.92	0.34	-1.99	-0.11	1.35	-0.69	3.57
4	0.63	0.21	2.89	0.13	2.22	-1.37	4.55
5	-0.41	-0.67	-0.93	-0.86	-4.79	-4.57	0.34
6	-1.99	-0.19	-2.15	-0.41	1.06	0.65	2.54

¹Target registration errors (TRE, in mm; last column) using all 27 markers available. The observed and estimated coordinate values (mm) are given in the central six columns.

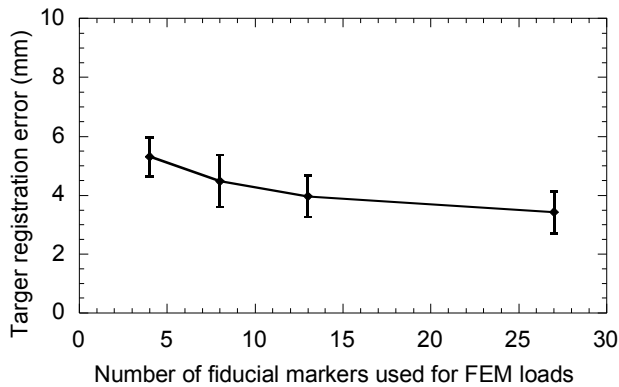


Fig. 7. Dependence of target registration error (TRE) on number of fiducial markers used in steady-state FEM model. Standard errors are shown based on six measurements for each point.

IV. DISCUSSION

The SSHT FEM model performs well for multimodality breast image co-registration, under the assumption that there are no stress-induced deformations. The co-registration, FEM-based procedure with external fiducial markers for multimodality breast imaging is accurate to within about 5mm.

V. REFERENCES

- [1] C. J. Baines (1998). "Menstrual Cycle Variation in Mammographic Breast Density". *Natl. J. Cancer Inst.*, 90, 875.
- [2] The Finite Element Method: Basic Concepts and Applications (Series in Computational and Physical Processes in Mechanics and Thermal Sciences), Hemisphere Publishing Corporation, 1992.